

AUTOMATIC DETECTION AND CLASSIFICATION OF LEUKEMIA FROM BLOOD SMEAR IMAGE USING SENET CONVOLUTIONAL NEURAL NETWORK

SHALINI V¹, K. S. ANGEL VIJI²

¹Research Scholar, Department of Computer Applications, Noorul Islam Centre for Higher Education, Thuckalay, Kumaracoil, Tamil Nadu, India

²Associate Professor, Department of Computer Science and Engineering, College of Engineering, Kollam, Kerala, India,

E-mail: ¹shalinijewel@gmail.com, ²ksangelviji@gmail.com

ABSTRACT

Leukaemia is a subtype of blood cancer that manifests itself by excessive production of abnormal blood cells. Leukemia is on the rise, and it takes more time to diagnose and treat because of the disease's high mortality rate. One such disease is leukaemia, which affects the white blood cells. Early, reliable, and safe detection of leukaemia dramatically improves treatment and survival rates. Pre-processing, segmentation, extraction of features, and the leukaemia classifier are the four components of the classification methodology. Using a hybrid Squeeze-and-Excitation Networks (SENet)-based CNN (convolutional neural network), this work can identify ALL (acute lymphocytic leukaemia), CML (chronic myeloid leukaemia), CLL (chronic lymphocytic leukaemia) and AML (acute myeloid leukaemia) in this study. The proposed SENet-CNN model detects the classification of four leukaemia subtypes, including ALL, AML, CLL, and CML, from blood smear images. The performance of the proposed SENet model is assessed using metrics like accuracy (ACC), specificity (SP), Precision, F1- score, and sensitivity (SE). The proposed model outperforms the other techniques by having a classification accuracy of 99.98%, according to experiments on a dataset of 655 images.

Keywords: *Leukemia Detection, SENet-CNN, Blood Smear Images, Deep Learning, Convolutional Neural Network, Segmentation and Classification*

1. INTRODUCTION

A deadly blood cancer known as leukaemia is characterized by aberrant and unchecked lymphocyte growth. Some of the elements of blood are RBC (red blood cells), platelets, and WBC (white blood cells). Leukemia is a procedure of cancer that arises from the cells that ordinarily give rise to different blood cell types. Leukemia most frequently begins as WBCs, although some leukaemias can also begin as other blood cell types. They divide leukaemia into acute (fast-growing), chronic (slow-growing), and those that begin in lymphoid or myeloid cells. Knowing the precise form of leukemia a patient has enables doctors to determine better their prognosis and the most appropriate course of treatment. According to the definition of "acute," leukaemia can advance quickly and result in death within months if left untreated. Lymphocytic refers to the fact that it originates from immature lymphocytes, a kind of WBC. Scotti et al. [1] have described an automated morphological technique's efficacy in recognizing acute lymphocytic leukaemia

in peripheral blood microscopy pictures. The suggested system separates leucocytes from other blood cells in the blood image first, assesses morphological indexes from those cells, then chooses lymphocyte cells (those targeted by acute leukaemia), and finally identifies the presence of leukaemia.

Mohapatra et al. [2] have proposed a procedure that first isolates leukocytes from other blood cells before removing lymphocytes from the subclass. Leukaemia detection is suggested using two additional features for determining cell nucleus boundary roughness. Rawat et al. [3] have proposed a method that helps to establish a computer-aided screening for AML and ALL and increases the diagnosis accuracy of AML and ALL by employing image processing to analyze colour, structural, and textural aspects of the blood image. This work aims to outline a quantitative microscopic method for separating malignant from normal blood smears. Rehman et al. [4] have projected a method for categorizing reactive bone marrow (normal) and ALL into their several subtypes in stained bone

marrow pictures. Ahmed et al. [5] have proposed a CNN architecture that can identify all leukaemia subtypes. In addition, this work also examined various support vector machines, k-nearest neighbors, decision trees, and additional well-known machine learning methods like naive Bayes. The following are the main contributions of this proposed model.

- The proposed methods are also tested on the ALL-IDB and ASH image group datasets.
- Pre-processing procedures are being applied to the blood smear photos, including image resizing and contrast boosting.
- The WBC nucleus is segmented in this learning by upgrading the nucleus and conquering the other parts of the input images.
- The extraction of traits, such as outline features, colour features, and surface features, comes next.
- On the other hand, the proposed work leverages complex SENet CNN architectures to categorize four leukaemia subtypes, including ALL, AML, CLL, CML, and healthy leukaemia.
- The proposed CNN based on deep learning (DL) and the hybrid of SENet thereby exceed the current techniques with 99.98% accuracy, as demonstrated in the results section.

The remainder of the manuscript is structured as follows: The rest is divided into the following sections: The associated works are outlined in Part II. The suggested SENet for the techniques employed in this paper is presented in Part III. Part IV Experimental results are discussed. Finally, Part V summarises the conclusion.

2. RELATED WORK

Bindhu et al. [6] have described how images from diverse fields have been processed using the current digital image processing techniques. In this manuscript, we have covered a variety of applications, including image restoration and sharpening. Anwar et al. [7] have described an automated diagnostic method that uses identifies ALL using a CNN model. The model recognizes the malignant leukemia cells using labeled images of microscopic blood smears. Kumar et al. [8] have described systems that use artificial intelligence to help with decision-making in clinical settings and have great potential for identifying hematological malignancies. This research aims to create a DL-based system used to forecast the detection of acute

leukaemia in blood cell images. Anilkumar et al. [9] have proposed a study that describes a computer-aided diagnosis method that compares leukaemia images to normal images using deep convolutional neural networks (CNNs) that have been trained. [10] Anna Merino et al. [10] investigated systems that used artificial intelligence to aid in clinical decision-making and discovered that they have a high potential for detecting haematological malignancies.

Shalini et al. [11] have proposed that residual neural networks (RNN) are a variation of a neural network that has been changed once more to become ResNet-50. The raw image was processed using convolutional and max-pooling layers to extract the most features. Attea et al. [12] have proposed that CNN's hyperparameters and architecture to enhance classification performance are modified to the input data using the Bayesian optimization method. Tusar et al. [13] have put out an automated Deep Neural Network-based technique for recognizing various-shaped ALL blast cells from microscopic blood smear images (DNN). The technology can distinguish between several kinds of ALL cells with a 98 percent accuracy rate. Baig et al. [14] have employed DL-based CNN that combines CNN-1 and CNN-2 to detect ALL, multiple myeloma (MM), and AML. Using images of microscopic blood smears, the suggested model can identify malignant leukaemia cells [15 – 20].

2.1 Sections and Subsections

Sections and subsections should be numbered and titled as 1.0, 2.0, etc. and 1.1, 1.2, 2.1, 2.2, 2.2.1, etc. Capital letters should be used for the section titles. For subsections, the first letter of each word should be in capital letter and followed by small letters. One line space should be given above the sub section while no space should be given below the heading and text

2.2.2 Identification of sub subsections

Subsub section has to be in sentence case with no spacing above or blow the srat of it.

3. PROPOSED METHOD IS BASED ON SENET-CNN LEUKEMIA CLASSIFICATION

This segment defines the experimental setup accustomed conduct the investigation. The process of retrieving the dataset is first detailed, and then the SENet models that were used to categorize the different subtypes of leukaemia are explained. The general structure of the proposed hybrid SENet is provided in the following.

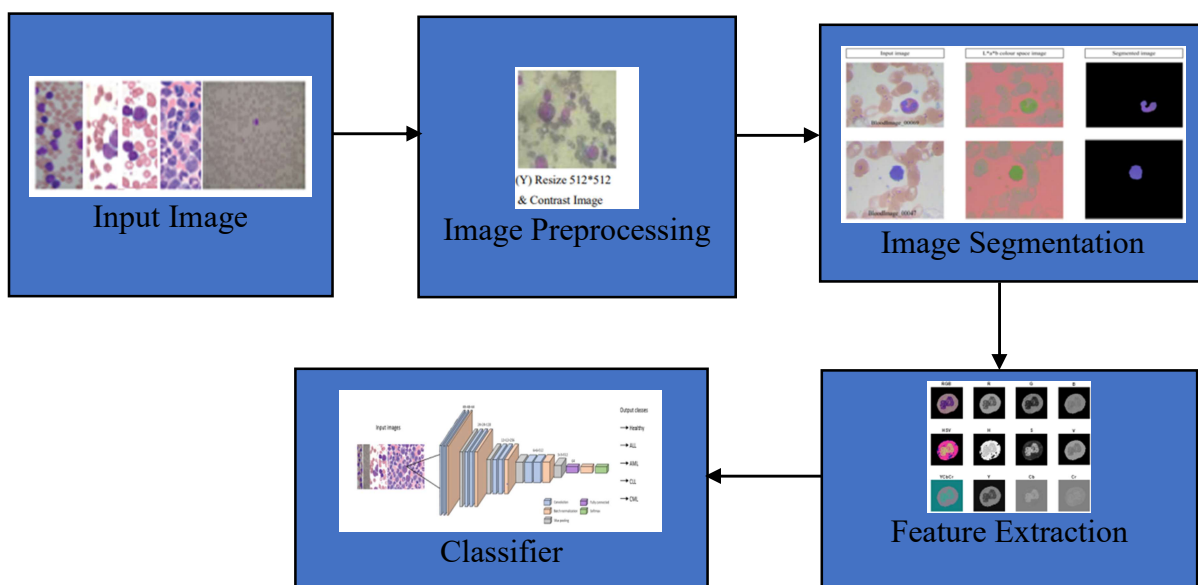


Figure 1. Block Diagram for the proposed SENet of leukemia classification

The proposed SENet-CNN of leukaemia classification flowchart is shown in Figure 1. Images of smear blood are segmented using k-means clustering, shape, texture and color feature extraction, and pre-processing for ALL, CLL, AML, and CML (image resizing and contrast). this work suggested research focuses on classifying two subtypes of leukaemia, especially ALL, AML, CLL, and healthy, by applying sophisticated SENet-CNN architectures.

3.1 Dataset

Description of the Leukaemia database. The two sources used to create the dataset are the ASH picture bank and ALL-IDB. A vast selection of images on a diversity of homological topics are offered by the ASH picture group, which is freely accessible online. This article's annotated blood leukaemia cell images were picked from all of the accessible ones, including any of the four subtypes. The ALL-IDB collection contains the blood smear photos with annotations. These images were pre-processed before being segmented, feature-extracted, and classified. The ALL-IDB only contains leukaemia's that are healthy and ALL leukaemia kinds. The ALL-IDB dataset does not reveal any of the remaining leukaemia subtypes. Competent oncologists gave each image in the collection the ALL categorization, making the ALL-IDB more regarded as a reputable source of information... This work makes use of colored blood

microscopic pictures from the ALL-IDB datasets. The two subsets are combined in the current study to supplement the data as a SENet model is trained on a hybrid dataset of blood smear images.

3.2 Image Preprocessing

Depending on the processing goal, there are two categories of pre-processing techniques: the first is image resizing, which includes sizes like 512*512, 256*256, and 128*128. The image's edges and small features can be successfully sharpened by combining the "fspecial" function with the "unsharp masking" filter. Use the "imfilter" function with the Boundary Option "replicate" to apply this filter to an image. With this selection, input array values that fall outside of the array's bounds are assumed to be comparable to the value closest to the array's edge as shown in Figure 2.

Table 1. Algorithm for unsharp Filtering for image pre-processing

Step 1	Image input is read (X).
Step 2	Use output Y = imresize (X, [512×512]).
Step 3	Use the unsharp masking filter to create a new variable with a color filter that has the same attribute as the input image.
Step 4	Apply the repeat boundary filter algorithm on Y Combine the three separately separated RGB planes.
Step 5	Combine the three planes into one.
Step 6	Output (Y)

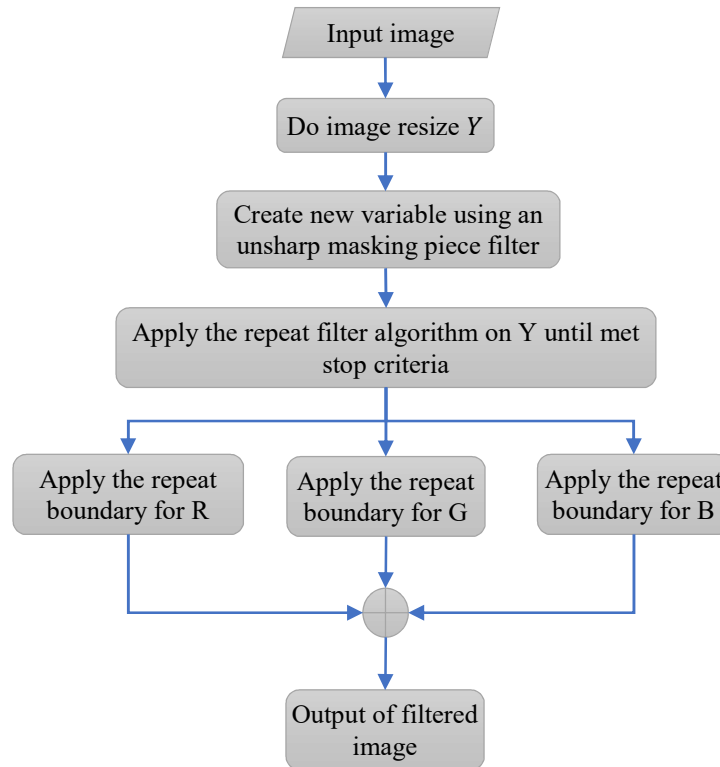


Figure 2. Flowchart of pre-processing process

3.3 Image Segmentation

An image of a WBC taken at a microscopic scale can have its nucleus extracted via leukocyte segmentation. It plays a crucial role because proper segmentation is necessary for adequate cell classification. All automated blood malignancy recognition and classification systems are built on it. The segmentation method employed in this work is k-mean cluster-based. Therefore, the leukocyte items of interest are divided in this step.

K-means clustering classifies n data points into classes (a_1, a_2, \dots, a_n) and into k clusters based on their inherent distance from one another. the k-means system sums the squared error function from equation (1) to find related intensity-based regions. It anticipates that they frame a vector space to find consistent huddling in the information features. Figure 3 describes the k-mean algorithm's operational flow diagram. The centroids are surrounded by a group of focal points $\mu_i \forall_i = 1 \dots k$.

$$L = \sum_{i=1}^K \sum_{a_j \in w_j} \|a_j - \mu_i\|^2 \quad (1)$$

With k clusters in $w_j, i = 1, 2, 3, \dots, k, \mu_i$ are the centroid of all the points $a_j \in w_j$. The algorithm iteratively minimizes the j -th criterion function. Image segmentation Using K-means clustering steps are given below

Step 1 Determine the intensity histogram.

Step 2 Set the centroids' intensities at random intervals of k .

Step 3 When the cluster labels in the image stop changing, keep on by repeating the next few steps.

Step 4: Group the points based on how far the points are from the centroid intensities.

$$C^i = \arg \min_j \|a_j - \mu_i\|^2 \quad (2)$$

Step 5 Calculate each cluster's new mean or centroid.

$$\mu_i = \frac{\sum_{i=1}^m 1\{c^i=j\} a^i}{\sum_{i=1}^m 1\{c^i=j\}} \quad (3)$$

where k is the complete quantity of clusters, j is the complete number of iterations for every one of the cluster centers, and I is the number of iterations over the strengths, and i is the mean intensity utilized, Segmentation of white blood cells was performed with K-means that use the nucleus region identification of white cells method, as displayed in Figure 2. The nucleus can be separated from the backdrop in $L^*a^*b^*$ colour space by employing the k-means clustering technique. Depending on its a^* and b^* values, every pixel in an object is separated into one of two groups in the $L^*a^*b^*$ color model.

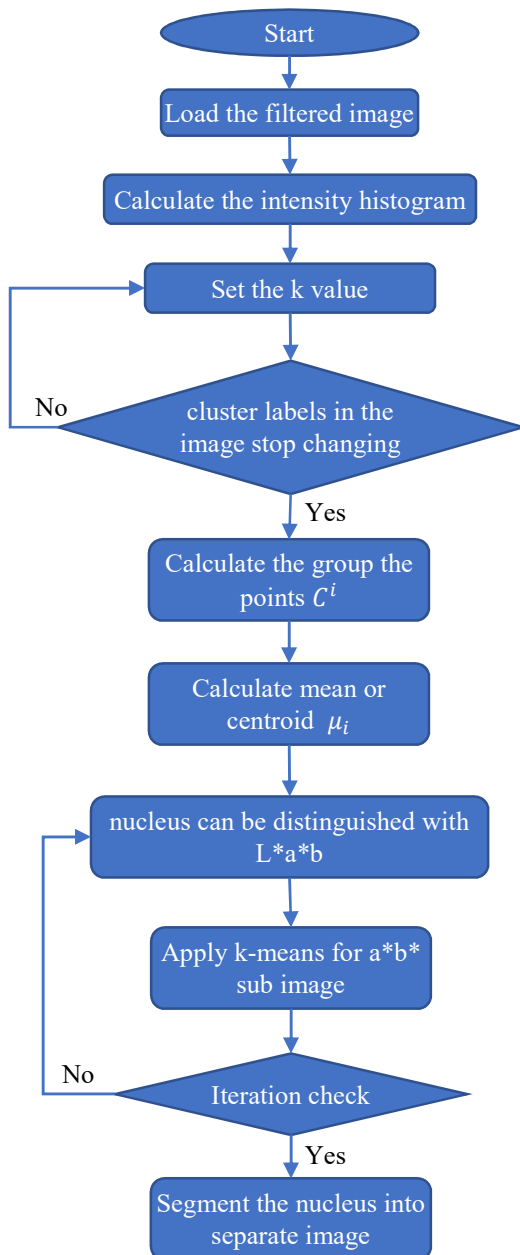


Figure 3. Flowchart Of Proposed K-Means Cluster-Based Nucleus Segmentation

3.4 Feature Extraction

In image processing, feature extraction entails using less resources to describe a huge quantity of data. Shape features, texture features, and fractal dimension are the four main categories of characteristics retrieved in the current research. The nucleus image is also used to extract colour characteristics.

A) Shape Feature: - The haematologist claims that the nucleus's shape is crucial for identifying blasts. Obtaining boundary- and region-based shape features for the examination of the

nucleus' shape. The nucleus' binary equivalent picture is used to extract all of the characteristics, with nonzero pixels used to represent the area around the nucleus. Using the properties that were retrieved from the two classes, region- and boundary-based, this work performs a quantitative evaluation for each nucleus. These characteristics are as follows:

Area: It was determined how many pixels overall in the image region were none zero.

Perimeter: By computing the distance between the subsequent boundary pixels, the perimeter was determined.

Compactness: The definition of a nucleus's compactness or roundedness is given in (4).

$$Compactness = \frac{Perimeter^2}{Area} \quad (4)$$

Solidity: The solidity of a blast cell is determined by the ratio of the convex hull area to the actual area, another important factor in blast cell classification. This standard is explained in (5).

$$Solidity = \frac{Area}{ConvexArea} \quad (5)$$

Eccentricity: The amount a nucleus deviates from a circular form is measured using this metric. It is an important trait because lymphocytes are more rounded than blasts. Defining a relationship in order to measure this (6).

$$Eccentricity = \frac{\sqrt{a^2 - b^2}}{a} \quad (6)$$

Elongation: Nucleus bulging that is out of the ordinary is another sign of leukaemia. As a result, the nucleus bulging is expressed as a ratio known as the elongation. The formula for this quantity, known as the ratio of the greatest to minimum distances (Rmax and Rmin) from the center of gravity to the nucleus border, is as follows: (7).

$$Elongation = \frac{R_{max}}{R_{min}} \quad (7)$$

Form factor: This parameter, which has no dimensions and fluctuates in response to surface imperfections, is described as (6)

$$Formfactor = \frac{4 \times \pi \times Area}{perimeter^2} \quad (6)$$

B: Texture Feature:- The nucleus pictures were converted to a grey scale for the nucleus texture measurements. The co-occurrence matrices for each nucleus picture were used to determine these characteristics that includes:

Homogeneity: This idea refers to how diverse something is.

Energy: Uniformity is measured using energy.

Correlation: This shows how the values of the pixels are related to their surroundings.

Entropy: Entropy is a commonly used indicator of unpredictability.

Contrast: As a whole, contrast is a measurement of the difference in intensity of both a given pixel and its neighbouring pixels.

C. Extraction of Color Features: Color is taken into account while extracting features from nucleus regions since it is an important component of human perception during visual perception. As a result, the mean color standards in the RGB and HSV color spaces are calculated for each nucleus image. It is specified in accordance with a specific model or colour space. YCbCr, HSV, RGB, and other color spaces have all been utilized to make it simpler to extract the features. Information can be gleaned from the blood cell image using its color features to categorize it correctly.

3.5 Proposed SENet CNN classification

In this part, this work also outline this work proposed CNN architecture and a technique for facial sentiment recognition. Convolutional layers are carefully chosen with respect to neuron counts in CNN's architecture to deliver the best performance possible. There is typically no set standard criterion for choosing a convolutional layer with a certain number of neurons.

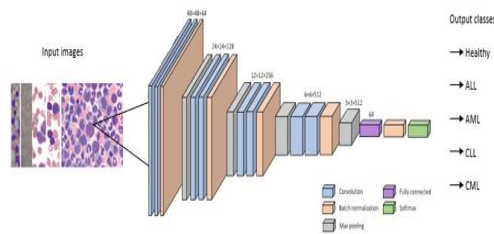


Figure 4. Architecture of Proposed SENet Convolutional Network.

SENet is a shallow CNN architecture that this work have however implemented. The 48 X 48 or 128 X 128 input moves through four convolutional blocks before arriving at a fully connected layer, as illustrated in Figure 4, which is a rather simple representation of the SENet Convolutional Network architecture. The batch normalization layer and the pooling layer come after the two subsequent convolution layers of the convolutional block. The completely linked layer and each convolution block are followed by a dropout layer. The SoftMax layer is then employed for classification. The following sections provide descriptions of the various layers and activation functions.

3.5.1 Convolution Layer

Processing the image's high-level features using the convolutional layer is the fundamental element or building block of CNNs. Edges, colours, and textures are examples of relatively low-level

characteristics that are often extracted by the first convolutional layer, whereas the following layers typically extract high-level features. The forward-backward propagation approach is used to recover important information from the input image using the convolution kernel. This work concatenated 64 to 512 kernels from various convolutional blocks in order to create 3X3 convolutional kernels in all of the convolution layers of this work network architecture. After every convolutional block, a batch normalization layer is added to lessen the interior covariate shift and quicken the training process.

3.5.2 Activation Function

Which node in the convolutional neural network design should be active is determined, and the activation function selects nonlinear features to be added to the model. Activation functions come in a wide variety of forms, but in this work work, this work choose the ReLu, or recited linear unit, activation function that is most frequently utilized. The mathematical formula for ReLu is

$$ReLU(x) = \max(0, x) \quad (7)$$

where x denotes a neuron's input

3.5.3 Pooling layer Pooling

These speeds up CNN training and lowers the computational cost. This study outputs the maximum value from the 2 x 2 window using Max-pooling. This window moves with a 2 stride size on the convolutional feature map. The resulting dimension can be determined using the formula below:

$$M_o = \text{floor} \left(\frac{M_i - F}{S} \right) + 1 \quad (8)$$

where the parameters M_i , S , and F specify the kernel, stride, and respective sizes of the input image.

3.5.4 Fully connected layer

The last max-pooling layer's features map is used to first flatten the fully connected (FC) layer before it feeds into the FC. Within a filter size of 1 x 1, neurons from one layer are connected to neurons from another layer in this layer.

3.5.5 Dropout

Input elements are eliminated at random during training as part of the regularisation process known as "dropout" to avoid over-fitting. To prevent over-fitting issues and boost model effectiveness, this work employ a dropout of 0.35 after each convolutional block and after the fully connected layer.

3.5.6 SoftMax

Multi-class classification problems are resolved using the network's softmax layer, which is the top layer. The likelihood of each category in the target class with the highest probability is returned

by the softmax function 37. The SoftMax function's mathematical expression is provided by

$$\text{Softmax}(x_i) = \frac{\exp(x_i)}{\sum_{j=1}^N \exp(x_j)} \quad (9)$$

where N is the number of classes and xi are the inputs from the previous layer for each SoftMax layer.

SENet: A fundamental structural idea for CNNs, networks strengthen channel connectivity. As can be seen in Figure 5, which depicts how SENet operates, this drastically cuts down on the computational cost to nearly nothing. The graphic shows the number of channels and the function provided as input to a convolutional block, with the values from each channel averaged to a single value. Using SENet, the network can fine-tune the weighting of each feature map by appending a variable to each channel in a convolutional block. Here, the kernel is used as a weighting function, which is employed in non-parametric estimation procedures and by which the density functions of random variables may be estimated or the conditional expectation of a stochastic process can be estimated using kernel regression. Among the many feature descriptors available for use in computer vision and image processing for the aim of illness classification is the histogram of oriented gradients (HOG). Squeeze is one half of the embedding structure used to assign channel-level feature weights in the SENet network. The channel-level global feature \mathbb{F} was calculated by averaging the data from the feature space fs to a single value.

$$f_{S_C} = \mathbb{F}_{\text{squeeze}} \left(\sum_{i=1}^{\text{Width}} \frac{1}{\text{Width} \times \text{Height}} \right) \quad (10)$$

Excitation is the final half, and it is realised by two layers that are joined end to end. To speed things up, the first FC layer wrappings \mathbb{C} channels into $\frac{\mathbb{C}}{r}$ channels, while the second layer recovers \mathbb{C} channels and r represented as the density ratio. Allocating the learnt channel correlation analysis to each channel after the model has learned the correlation between channels is an efficient method of training the model to prioritise the characteristics of the relevant channels. As a result, \mathbb{S} is being used to hide such minor channel details.

$$\mathbb{S} = \mathbb{F}_{\text{Excitation}}(f_{S_C}, \text{Width}) \quad (11)$$

The transitional characteristics of the image were finally downsampled using the maximum pooling layer. The eventual classification of the involvement leukemia images as ALL, CLL, AML, and CML was accomplished by feeding the results of the pooling process into the final two layers, such as the FC layer and the softmax layer.

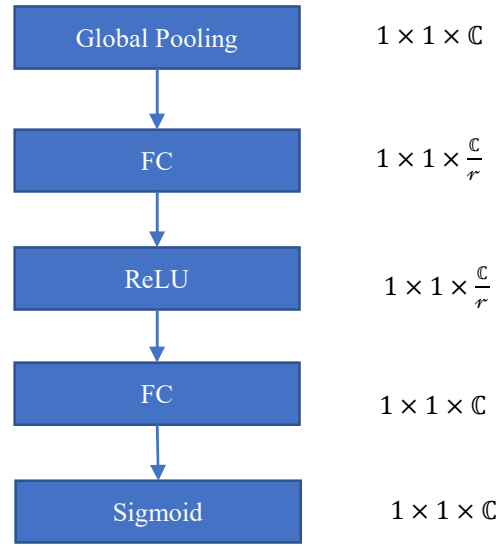


Figure 5. SENet Block

3.6 Performance metrics

To evaluate the proposed recognition and categorization model, the authors use disease-related statistical metrics such as specificity, recall, accuracy, precision, and F1 score. Classifications with a positive outcome are denoted by TP rate (true positive), FP rate (false positive), TN rate (true negative), and FN rate (false negative). Conversely, the recall of a leukaemia subtype class is a measure of how well it can be predicted. Predictions of known subtypes of leukaemia are consistent with the actual subtypes. The F1 score is the transfer function of the recall and accuracy metrics, whereas precision is the fraction of projected positive leukaemia subtype classes that were really correct. To test the model, it is necessary to assess additional performance metrics. These actions are briefly defined as

Accuracy: This metric determines how well a method performs by calculating how many accurately anticipated examples there are overall. It is written mathematically as follows:

$$\text{Accuracy} = \frac{TP+TN}{TP+FP+TN+F} \quad (10)$$

Precision: Precision is the ratio of all instances of positively predicted events that came true to all positively anticipated events. Low false positive rate and high precision are connected. As stated in the following manner:

$$\text{Precision} = \frac{TP}{TP+FP} \quad (11)$$

Specificity: The ratio of all accurately negative observations to all situations in a negative position determines the outcome. This measure shows how often dissimilar infection types are appropriately classified.

$$\text{Sepecificity} = \frac{TN}{TP+FP} \quad (12)$$

Recall: This ratio represents the proportion of appropriately forecast positive explanations to all of the actual class's observations.

$$(Recall) \text{ sensitivity} = \frac{TP}{TP + FN} \quad (13)$$

F1 score: One of the mutual criteria for evaluating a classifier's performance is the F1 score. The F1 score is an appropriate measurement for classification problems on instable data sets meanwhile it is supplementary delicate to data circulation.

$$F1 - Score = 2 \times \frac{rec \times precis}{recall + precis} \quad (14)$$

4. EXPERIMENTAL RESULT AND DISCUSSION

The dataset combines the ALL-IDB and the ASH picture bank as its two sources. Figure 6 displays several examples of images from datasets. As a SENet-CNN model is trained on a hybrid dataset of blood smear pictures, the two subsets are blended in the current study to complement the data. The hybrid dataset has 655 blood smear images in total, including 159 photos of healthy blood and 149 images each of ALL, 104AML, 128CLL, and 115CML.

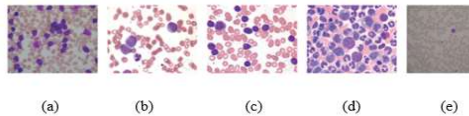


Figure 6. (a) ALL (b) AML (c) CLL (d) CML and (e) Healthy

4.1 Image pre-processing

The blood smear photos are put through pre-processing operations, including image shrinking and contrast boosting. such as 256 * 256, 128 * 128 and 512 * 512. Utilizing the "fspecial" function and the "unsharp masking" filter, Figure 7 demonstrates contrast improvement.

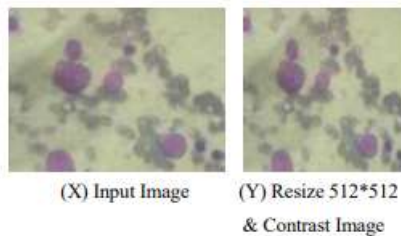


Figure 7. Preprocessing result output

4.2 Image segmentation

By enhancing the nucleus and overpowering the other parts of the blood smear pictures, the k-means clustering technique is employed in this study to segment the WBC nucleus. Each pixel of an object in the L*a*b* color space is split into four clusters according to the corresponding a* and b* values.

The segmented image's results are shown in Figure 8.

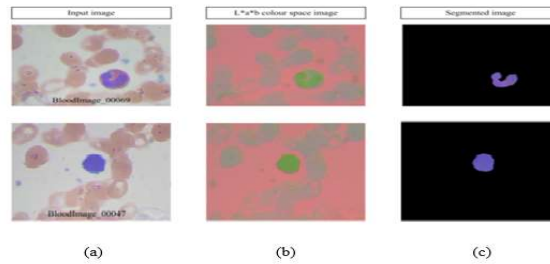


Figure 8. Segmentation using k-means clustering, (a) input images (b) L*a*b* colour space image and (c) final segmentation.

4.3 Feature extraction

The subsequent phase, Extracted Characteristics, included shape characteristics, texture features, and color features. YCbCr, HSV, RGB, and other color spaces have all been utilized to simplify extracting the features. Information can be gleaned from the blood cell image using its color features to categorize it correctly. Figure 9 shows color feature extraction

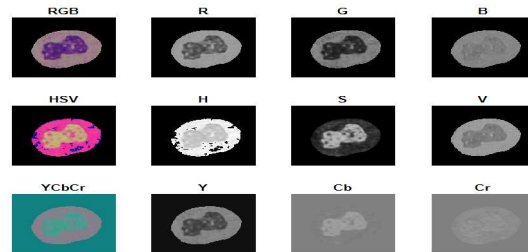


Figure 9. Color feature extraction

4.4 SENet classification

The proposed SENet-CNN model detects the classification of four leukaemia subtypes, including ALL, CLL, AML, and CML, from blood smear images. The presented models are evaluated using performance metrics like as precision, recall, F1 score, and accuracy. The benchmark dataset, ALL-IDB, and ASH image bank's F1 score, accuracy, precision, recall, and other metrics were calculated for each kind of leukemia. According to Table 2, the accuracy of the SENet-prediction CNN is 100% for ALL, CLL, CML, AML, and healthy patients. Additionally, the accuracy of the CNN's precision, recall, and F1 score are 100%, or 1.0, for all other cases. It is 99.91% accurate to predict CLL using SENet-CNN. However, all three metrics—accuracy, recall, and F1 score—are 0.99%. In contrast to SENet-prediction CNN's accuracy for CML, which is 98.96%, for AML, it is 98.99%, with precision of 0.99%, recall of 1.00%, and F1 score of

1.0%. For healthy and ALL, SENet-CNN predicts with 100% accuracy, precision, recall, and F1 score.

Table 2: Performance of the SENet-CNN model for classifying leukemia subtypes

Leukemia type	Precision	Recall	F1 score	Accuracy
ALL	1.0	1.0	1.0	100
AML	0.98	0.99	0.99	98.99
CALL	0.99	0.99	1.0	99.91
CML	0.99	1.0	1.0	98.96
Healthy	1.0	1.0	1.0	100

Figure 10 displays the performance of SENet-CNN in terms of leukemia subtype detection.

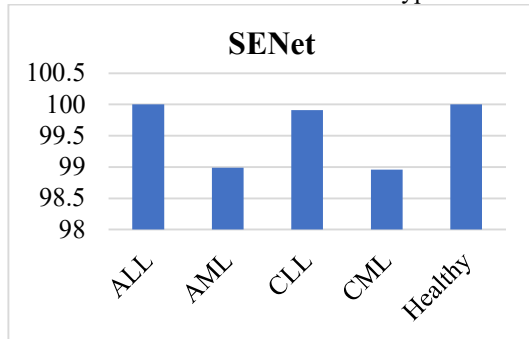


Figure 10: Accuracy of the SENet-CNN model for classifying leukemia subtypes

To illustrate their efficacy, the suggested models are compared to prior techniques like CNN [5] and GA with SVM [3]. ResNet50 is used to identify ALL and healthy samples, GA with SVM is used to identify ALL, AML, and healthy samples, and CNN is used to identify the specific kind of leukemia in each sample. However, Figure 12 shows that the used models, namely SENet-CNN, perform better than the current models, such as AlexNet, GA with SVM, CNN and ResNet 50. Figure 11 illustrates that the accuracy of ResNet 50 99.61%, GA with SVM is 99.50%, AlexNet is 99.41%, CNN is 81.74%, and SENet is 99.98%. As a result, SENet-CNN triumphs over the alternatives. The ASH image bank and All-IDB datasets were previously used to diagnose leukaemia and its subtypes using machine learning techniques.

Table 3. Comparison of accuracy with existing methodologies

Leukemia classification	Accuracy
AlexNet [6]	99.41
CNN [5]	81.74
GA with SVM [3]	99.50
ResNet 50 [11]	99.61
Proposed SENet-CNN	99.98

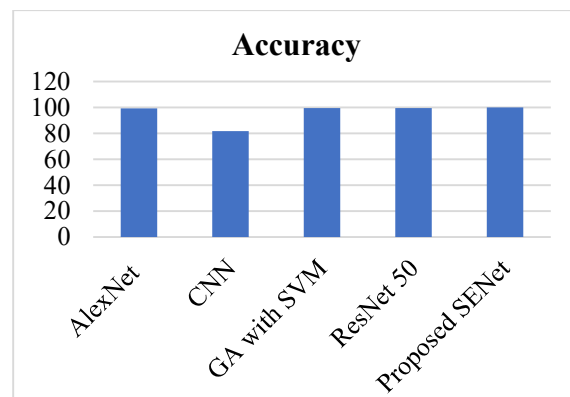


Figure 11. Comparison of leukemia classifier

Table 3 provides a complete assessment of the suggested models' accuracy compared to the earlier methods. Also shows that the proposed models perform better than the earlier methods, with an average accuracy of 99.98% for SENet-CNN.

5. CONCLUSION

In this study, the proposed SENet model detects the classification of four leukaemia subtypes, including AML, ALL, CLL, and CML, from blood smear images. The SENet-CNN models are used to determine the leukemia's diagnosis. Images of stained blood smears were segmented into WBC nuclei, and then the article extracted pertinent features to identify leukemia. The proposed SENet-CNN method's accuracy of 99.98% is more than that of the existing classification methods. The classification's effectiveness is compared to several techniques, including alexNet, CNN, GA with SVM, ResNet 50, and SeNet-CNN. The experiment results show that the SeNet method has outperformed conventional methods in terms of accuracy and other performance metrics. Results were obtained, including the sub-typing of leukemia to produce better performances.

REFERENCES:

- [1] Scotti, Fabio. "Automatic morphological analysis for acute leukemia identification in peripheral blood microscope images." In CIMSIA. 2005 IEEE International Conference on Computational Intelligence for Measurement Systems and Applications, 2005., pp. 96-101. IEEE, 2005.
- [2] Mohapatra, Subrajeet, Dipti Patra, and Sanghamitra Satpathi. "Image analysis of blood microscopic images for acute leukemia detection." In 2010 International Conference on Industrial Electronics, Control and Robotics, pp. 215-219. IEEE, 2010.
- [3] J. Rawat, A. Singh, B. Hs, J. Virmani, and J. S. Devgun, "Computer-assisted classification framework for prediction of acute lymphoblastic and acute myeloblastic leukemia," *BioCybernetics and Biomedical Engineering*, vol. 37, no. 4, pp. 637–654, 2017
- [4] Rehman, Amjad, Naveed Abbas, Tanzila Saba, Syed Ijaz ur Rahman, Zahid Mehmood, and Hoshang Kolivand. "Classification of acute lymphoblastic leukemia using DL." *Microscopy Research and Technique* 81, no. 11 (2018): 1310-1317.
- [5] N. Ahmed, A. Yigit, Z. Isik, and A. Alpkocak, "Identification of leukemia subtypes from microscopic images using convolutional neural network," *Diagnostics*, vol. 9, no. 3, p. 104, 2019
- [6] Bindhu, Dr. K. K. Thanammal, "Analytical Study on Digital Image Processing Applications," *SSRG International Journal of Computer Science and Engineering*, vol.7, no.6, pp. 4-7, 2020.
- [7] Anwar, Shamama, and Afrin Alam. "A convolutional neural network-based learning approach to acute lymphoblastic leukaemia detection with automated feature extraction." *Medical & biological engineering & computing* 58, no. 12 (2020): 3113-3121.
- [8] Kumar, Deepika, Nikita Jain, Aayush Khurana, Sweta Mittal, Suresh Chandra Satapathy, Roman Senkerik, and Jude D. Hemanth. "Automatic detection of white blood cancer from bone marrow microscopic images using convolutional neural networks." *IEEE Access* 8 (2020): 142521-142531.
- [9] Anilkumar, K. K., V. J. Manoj, and T. M. Sagi. "Automated detection of leukemia by pretrained deep neural networks and transfer learning: a comparison." *Medical Engineering & Physics* 98 (2021): 8-19.
- [10] Boldú, Laura, Anna Merino, Andrea Acevedo, Angel Molina, and José Rodellar. "A DL model (ALNet) for the diagnosis of acute leukaemia lineage using peripheral blood cell images." *Computer Methods and Programs in Biomedicine* 202 (2021): 105999.
- [11] V. Shalini, K. S. Angel Viji, "Integration of Convolutional Features and Residual Neural Network for the Detection and Classification of Leukemia from Blood Smear Images" *International Journal of Engineering Trends and Technology*, vol. 70, no. 9, pp. 176-184, 2022.
- [12] Atteia, Ghada, Amel A. Alhussan, and Nagwan Abdel Samee. "BO-ALLCNN: Bayesian-Based Optimized CNN for Acute Lymphoblastic Leukemia Detection in Microscopic Blood Smear Images." *Sensors* 22, no. 15 (2022): 5520.
- [13] Tusar, Md, Taufiqul Haque Khan, and Roban Khan Anik. "Automated Detection of Acute Lymphoblastic Leukemia Subtypes from Microscopic Blood Smear Images using Deep Neural Networks." *arXiv preprint arXiv:2208.08992* (2022).
- [14] Baig, Raheel, Abdur Rehman, Abdullah Almuhaimeed, Abdulkareem Alzahrani, and Hafiz Tayyab Rauf. "Detecting Malignant Leukemia Cells Using Microscopic Blood Smear Images: A Deep Learning Approach." *Applied Sciences* 12, no. 13 (2022): 6317.
- [15] Anilkumar, K. K., V. J. Manoj, and T. M. Sagi. "Automated detection of b cell and t cell acute lymphoblastic leukaemia using DL." *Irbm* 43, no. 5 (2022): 405-413.
- [16] Ghaderzadeh, Mustafa, Azamossadat Hosseini, Farkhondeh Asadi, Hassan Abolghasemi, Davood Bashash, and Arash Roshanpoor. "Automated detection model in classification of B-lymphoblast cells from normal B-lymphoid precursors in blood smear microscopic images based on the majority voting technique." *Scientific Programming* 2022 (2022).
- [17] Sujithraa, Gladys Saro, S. Karthigaiveni, S. Janani, and Hymlin Rose SG. "Use of Alexnet Architecture in the Detection of Bone Marrow White Blood Cancer Cells." *ECS Transactions* 107, no. 1 (2022): 5587.
- [18] Vijitha S and Sreelaja Unnithan N. "Modified Leading Diagonal Sorting with Probabilistic Visual Cryptography for Secure Medical Image Transmission." *Journal of Computational Science and Intelligent Technologies*, vol. 3, no. 3 (2022): 01-13. <https://doi.org/10.53409/MNAA/JCSIT/e202203030113>

- [19] Srikanth G N and M K Venkatesha. "Performance Analysis of AI Models for Audio Digit Utterance Detection." *Journal of Computational Science and Intelligent Technologies*, vol. 3, no. 3 (2022): 14-29. <https://doi.org/10.53409/MNAA/JCSIT/e202203031429>
- [20] T. Rajendran, K. P. Sridhar, S. Manimurugan, S. Deepa. "Advanced algorithms for medical image processing." *The Open Biomedical Engineering Journal*, vol. 13, no. 1 (2019): 102.